EUROFUSION WPJET1-CP(16) 15145

J Hillesheim et al.

Role of stationary zonal flows and momentum transport for L-H transitions in JET

Preprint of Paper to be submitted for publication in
Proceedings of 26th IAEA Fusion Energy Conference

Role of stationary zonal flows and momentum transport for L-H transitions in JET

J.C. Hillesheim[1], E. Delabie[2], E. R. Solano[3], F. Rimini[1], J. Hobirk[4], M. Barnes[5,1], J. Buchanan[1], C.F. Maggi[1], H. Meyer[1], L. Meneses[6] and JET Contributors*

EUROfusion Consortium JET, Culham Science Centre, Abingdon, OX14 3DB, UK
[1]CCFE, Culham Science Centre, Abingdon, Oxon OX14 3DB, United Kingdom
[2]Oak Ridge National Laboratory, Oak Ridge, Tennessee, USA
[3]Laboratorio Nacional de Fusiòn, CIEMAT, Madrid, Spain
[4]Max-Planck-institut fur Plasmaphysik, Garching, Germany
[5]Rudolf Peierls Centre for Theoretical Physics, University of Oxford, Oxford, UK
[6]Instituto de Plasmas e Fusao Nuclear, Instituto Superior Tecnico, Universidade de Lisboa, Lisboa, Portugal

Corresponding Author: jon.hillesheim@ukaea.uk

Abstract:
Recent experiments in JET, with an ITER-like W/Be wall, have investigated the role of stationary zonal flows and momentum transport for development of the edge transport barrier and dependencies of the transition from L-mode to H-mode. Studies have focused on ITER relevant factors including pushing towards small ρ^* with experiments at high toroidal magnetic field (3.0-3.4 T) and plasma current (2.2-3.2 MA), spanning $q_{95} \approx 2.7 - 3.9$, and characterizing the role of momentum transport and rotation in plasmas with high values of the L-H power threshold. We find that the radial wavelength of stationary zonal flows scales with the radial correlation length of turbulence, and that the radial correlation length of turbulence in cases where stationary zonal flows have been observed is several times smaller than the width of the edge radial electric field well. After NBI heating is added the inner shear layer of the well builds up into the core at constant gradient, while the outer shear layer moves inward. Linear gyrokinetic simulations show large growth rates over a broad range of spatial scales over the region where the flow shear increases at constant gradient.

1 Introduction

The conditions that permit access to H-mode continue to be one of the most significant uncertainties for operation of high performance plasmas in ITER, particularly in early

---

*See the author list of "Overview of the JET results in support to ITER" by X. Litaudon et al. to be published in Nuclear Fusion Special issue: overview and summary reports from the 26th Fusion Energy Conference (Kyoto, Japan, 17-22 October 2016) campaigns where available heating power will be limited. Subsequent to the installation of the ITER-like W/Be wall in JET, experiments studying the L-H transition have found typically lower threshold power in comparison to the carbon wall [1], dependencies on divertor configuration and SOL conditions [2–4], increased threshold with impurity seeding [3, 5], and I_p dependence in the low density branch of the transition [3]. Stationary zonal flows have also been observed during formation of the edge transport barrier in JET [6, 7].

We report in this paper on recent experiments investigating the role of stationary zonal flows and momentum transport in JET. Rather focusing on transition dynamics, we take the perspective of investigating which conditions in the plasma edge are important for barrier formation and what physical parameters and spatial scales may be important. Expanding on results in [6], edge zonal flows and the edge radial electric field well have been experimentally characterized in a second divertor configuration – the same used for high performance scenarios in JET – and during variations of plasma current and q_{95}. It is found that in cases where stationary zonal flows are observed that the radial correlation length of turbulence is several times smaller than the width of the edge E_r well. This could explain why the stationary zonal flow behavior is observed in JET, instead of oscillatory zonal flows observed in other experiments [8–12]. The role of momentum transport and rotation has been studied with gyrokinetic simulations, which show that the build up of the inner shear layer into the core at constant gradient cannot be attributed to critical gradient behavior for a flow shear driven instability.

2 Experimental methods

L-H transition experiments in JET are typically performed by slowly increasing the duty cycle of NBI sources or ramping the ICRH power, such that the input auxiliary heating power to the plasma increases by about 1 MW/s. Figure 1 shows time traces of NBI power, line-averaged density, plasma current, and on-axis toroidal magnetic field for a series of JET pulses in a density scan of the L-H transition threshold.

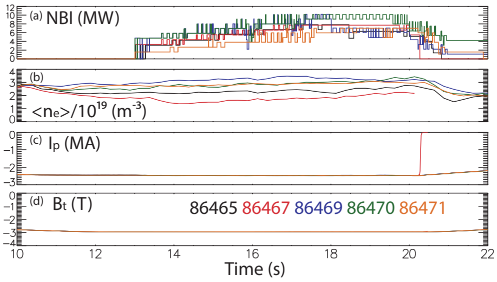

FIG. 1: Time traces showing (a) NBI power, (b) line-averaged density, (c) plasma current, and (d) on-axis toroidal magnetic field.

L-H transition studies reported in [6] used a vertically up-shifted plasma, with the strike points on the vertical target plates. This made Doppler backscattering (DBS) measurements possible with the antenna line-of-sight available at that time, which was designed for normal incidence reflectometry measurements. A new antenna, with a second line-of-sight was installed in 2015 along with upgraded digitizers. The first upgrade made DBS measurements possible in JET divertor configurations where the strike points are in the corners near the cyropump opening, or when configurations with the outer strike point on the horizontal target are used. The upgraded digitizers enabled the aliasing issues encounter in [6] to be avoided.

3 Characterization of P_{LH} at high plasma current and magnetic field

Figure 2 compares the results for L-H power threshold in Corner (C/C) divertor configuration, VT, and HT pulses. All Corner and VT pulses are 3.0 T/2.5 MA, while HT pulses were 3.0/2.5-2.75 MA. The thermal loss power, P_{lth}, is all auxillary heating, plus Ohmic heating, minus the time derivative of the stored energy and charge exchange losses. Data is shown both with and without estimated core radiation, P_{rad}, subtracted; in some cases the gas injection module used for fueling can interfere with bolometry measurements and P_{rad} can be an overestimate. Future analysis including tomographic reconstructions may change the estimated value of P_{rad}. Pulses at low density that depart from the high density branch show larger variation due to radiated power. C/C and VT show similar values for P_{LH} in the high density branch, but HT is significantly lower. This is similar to previous results [2–4]. It is notable that pumping efficiency is best in C/C and scrape-off layer densities are lower, compared to VT or HT, while X-point height is similar for C/C and HT, but higher for VT. Also global confinement in H-mode is typically best in Corner, so there does not appear to be a comparable correlation between the ratio of input power to P_{LH} and confinement across different divertor configurations.

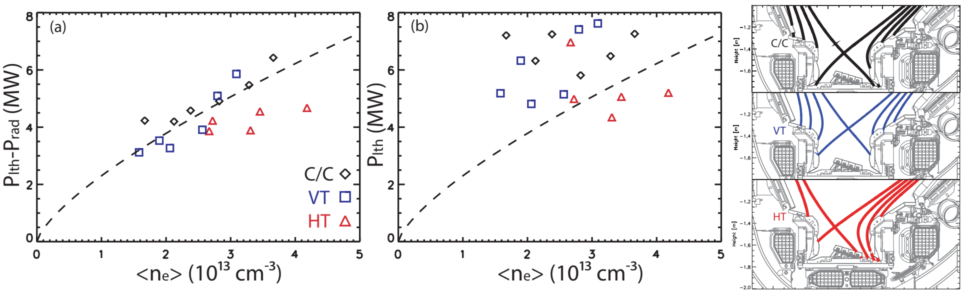

FIG. 2: Results for L-H power threshold comparing 3 divertor configurations at high magnetic field and current, $B = 3.0$ T *and* $I_p = 2.5 - 2.75$ MA, *both with estimated core radiation (a) subtracted and (b) included. Dashed lines are [13] scaling law predictions. Panel at right shows equilibrium reconstructions of divertor area.*

Figure 3 shows the results for plasma current and magnetic field scans in both the low and high density branch of the transition, for plasmas all in Corner divertor configuration.

Plasmas with the strike points in the corners are used for both “baseline” and “hybrid” high performance plasmas in JET due to improved pedestal pressures achieved and better power exhaust handling capabilities. A low triangularity shape similar to that used in JET “baseline” plasmas was used in the experiment, investigating dependencies of the L-H transition power threshold at high on-axis toroidal magnetic field ($B_t = 3.0 - 3.4$ T) and plasma current ($I_p = 2.2 - 3.2$ MA), covering edge safety factor values $q_{95} \approx 2.7 - 3.9$. Matching to the VT results, a density scan was performed at 3.0 T/2.5 MA. Then at two density values, one each in the high and low density branch of the L-H transition, B_t and I_p were scanned shot-to-shot to create a data set with pairs of shots where either q_{95} was held constant while B_t and I_p were increased, or where I_p was held constant when B_t was increased. Additional values of I_p were also acquired at constant magnetic field to cover a range of q_{95}. In the low density branch, the power threshold increases with plasma current at 3 T, but not at 3.4 T; this may be due to a combination of strong I_p dependence of P_{LH} in the low density branch and dependence of the density minimum on I_p. In the high density branch, there appears to be an unexpected departure from the L-H transition scaling law [13], which does have any plasma current dependence; [1] found a weak I_p dependence in JET-ILW. Instead, data show high P_{LH} at $q_{95} \approx 3$ at both 3 T (2.8 MA) and 3.4 T (3.2 MA). It should be noted that Z_{eff} was fairly high for these discharges, $\sim 1.8 - 2.1$, and bolometry data may have been affected by fueling, as mentioned above, and future tomographic reconstructions may change the values. The effect is reduced when the estimated radiated power is subtracted; however, since the ITER baseline scenario operates at $q_{95} = 3$ this effect should be investigated further. Figure 3(d) compares the experimental data to the 2008 scaling law predictions, both with and without estimated radiation subtracted. The low density, low current cases fall below the scaling law. The highest threshold cases do tend to fall above the scaling law predictions, even accounting for estimated core P_{rad}.

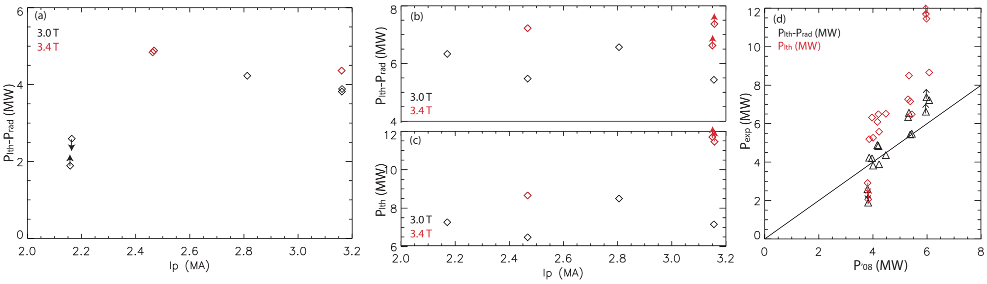

FIG. 3: Variation of L-H transition power threshold with plasma current and magnetic field, both in the (a) low density branch and (b-c) high density branch of the transition. (d) Comparison of all high current and field data to [13] scaling law, both with and without estimated core radiation subtracted. All have strike points in divertor corners. Arrows indicate upper or lower bounds.

4 Stationary zonal flows during development of the edge transport barrier

Expanding on the DBS measurements during development of the edge transport barrier previously acquired only in VT, Fig. 4 shows results during the Ohmic phase of pulses, where edge zonal flows were most clearly observed in previous experiments. Fine-scale structures in the edge flows are observed, but are less periodic in character than the previous measurements in VT, which could be related to differences in density profiles in the vicinity of the separatrix. Perhaps more notable in this data set is the variation of the width of the edge E_r well with plasmas current. For the current scan at constant magnetic field of 3.0 T, there is a systematic increase of the width of the edge radial electric field well with plasma current. At 3.4 T the width does not change, but there are changes in the SOL, in particular the appearance of a second well feature, which could also be important. The edge electron temperature increases substantially during the current scan. The edge ion temperature is within uncertainties of the electron temperature during L-H transition experiments in JET-ILW. The temperature approximately doubles from 2.2 to 3.2 MA, such that the banana orbit width changes marginally. The well width during Ohmic conditions may be related to large orbit effects and loss mechanisms in the edge, which would require detailed comparison to identify specific mechanisms. However, this data demonstrates that the edge well width clearly changes across the current scan, in some cases independently of the fine-scale structure.

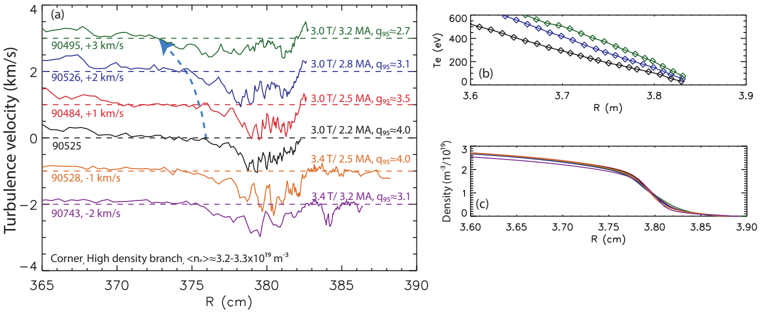

FIG. 4: (a) Edge turbulence velocity during plasma current and magnetic field scans, in high density branch of L-H transition. (b) Edge electron temperature measured with an ECE diagnostic for subset of current scan and (c) density profile measured with a profile reflectometer. Profiles radially shifted for consistent alignment.

Figure 5 compares the radial wavelength of the zonal flow structures with the radial correlation length of the turbulence, measured via correlation analysis of the two DBS channels. Although there is no clear scaling of the zonal flow wavelength with local gyroradius or collisionality, the zonal flow wavelength does correlate with the radial correlation length of the turbulence, and there are of similar size. Both radial scales are smaller than the width of the well; also, as shown in Fig. 4 the fine-scale structure and well width can scale independently of each other. This could explain why the fine-scale zonal flow structures are observed in JET, but have not been observed in smaller experiments with similar diagnostics. For their observation it might be a necessary condition that the radial correlation length of turbulence is significantly smaller than the well width – planned upgrades for DBS at JET to cover a broader frequency range should make this hypothesis testable in the future by enabling measurements at lower B_t.

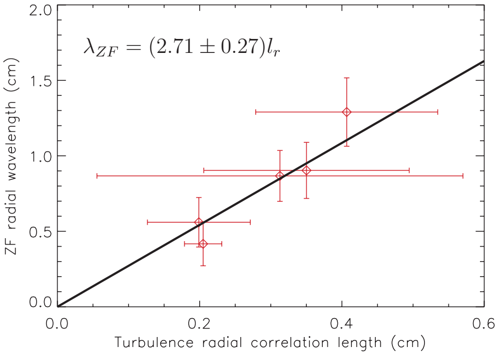

FIG. 5: Comparison of edge zonal flow wavelength, λ_{ZF}, to the radial correlation length of turbulence, l_r.

5 Influence of momentum transport and rotation during L-H transitions

In addition to the independent scaling of radial correlation length and well width, it was shown in [6] that there can be initial reduction in turbulence fluctuation amplitude due to development of a region of large flow shear in the edge before the L-H transition. These raise the question of how momentum transport affects the development of the edge radial electric field well, and by what degree the well is influenced by toroidal rotation. Figure 6 shows the development of the edge radial electric field well from Ohmic to L-mode conditions after NBI is added from the VT experiment, at densities below, near, and above the minimum of the L-H transition dependence on density. Several effects appear to influence the width of the well. Dashed lines are added to each panel, at the same slope, to show the development of the inner shear layer of the well, which builds inward at a constant gradient that is the same at all three density values. Density dependent behavior is observed for the outer side of the well. For the higher two densities, after NBI power is added the outer side of the well moves inward, and then does not change. The lowest density shows more gradual change, only moving inward after several hundred milliseconds. At the highest density, only part of the outer shear layer moves inward, unlike the lower two where the whole shear layer moves inward.

Figure 7 shows linear calculations performed with the GS2 gyrokinetic code. Calculations are done for a case near the density minimum, which falls on the high density branch, over radii where the flow shear is observed to build up at a constant gradient. The fastest

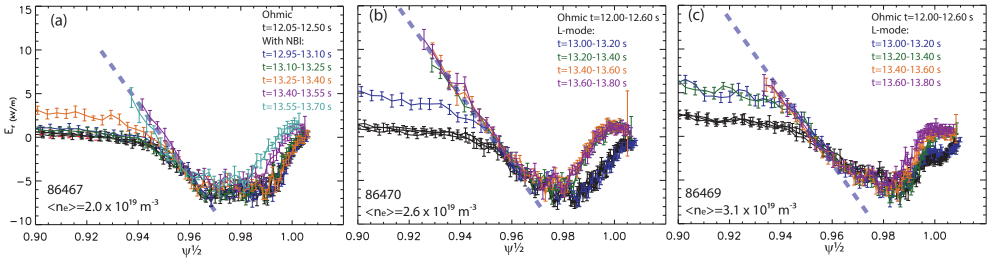

FIG. 6: Development of the edge radial electric field in three pulses, one (a) in the low density branch of the L-H transition (b) near the density minimum, and (c) in the high density branch. Profiles truncated when aliasing starts to impact DBS data. Dashed lines at the same slope added for visual aid.

growing mode at outer radii propagates in the electron diamagnetic drift direction, with the frequencies decreasing towards zero at inner radii. Growth rates are observed to be large of a broad range of spatial scales, increasing at high wavenumbers. Parallel velocity shear was scanned from zero to above the experimental value and negligible impact was found on linear growth rates, which shows that the apparent critical gradient value observed at radii where the toroidal flow is building up at a constant gradient does not arise due to a velocity shear driven instability. Non-linear simulations may give insight into how the apparent critical gradient behavior is related to momentum transport in the edge, but the high growth rates over a broad range of wavenumbers have made non-linear simulations difficult.

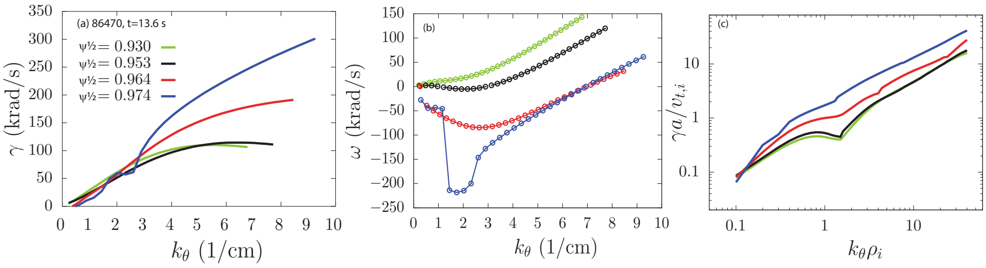

FIG. 7: Linear GS2 calculations of (a) long wavelength growth rates and (b) frequencies (negative is electron diamagnetic drift direction), (c) high-k growth rates.

6 Summary

We have reported on studies of the L-H transition focusing on ITER relevant aspects including operational parameters pushing towards small normalized gyroradius, ρ^*, with experiments at high magnetic field and current, and aimed at understanding the role of momentum transport and rotation on the development of the edge transport barrier, at high P_{LH}. It is found that the radial correlation length of turbulence is smaller than the width of the edge radial electric field well, and that the width of the well and fine-scale flow shear structures can scale independently of each other. This ratio of the radial correlation length to the well width could play an important role as an effective ρ^* for the L-H transition and development of the edge transport barrier, which could explain why a variety of phenomenology involving oscillating zonal flows and limit cycle behavior is observed in smaller experiments, but the stationary zonal flows are seen in JET at high B_t. Momentum transport limits the development of the inner shear layer and well width, and may be increasingly important for plasmas with high power threshold and heated with NBI, where large rotation shear is driven well before the L-H transition. Linear gyrokinetic calculations show that velocity shear-driven instabilities do not cause the apparent critical gradient behavior. Together this set of results investigating possible edge ρ^* effects and momentum transport show that there may be qualitative differences, particularly when the radial correlation length of turbulence is smaller than the well width, that start to be important at small ρ^*.

Acknowledgments

This work has been carried out within the framework of the EUROfusion Consortium and has received funding from the Euratom research and training programme 2014-2018 under grant agreement No 633053. The views and opinions expressed herein do not necessarily reflect those of the European Commission.

References

[1] C.F. Maggi *et al.*, Nucl. Fusion **54** 023007 (2014).
[2] H. Meyer *et al.*, *Proceedings of* 41^{st} *European Physics Society Conference on Plasma Physics*, P1.013 (2014).
[3] E. Delabie *et al.*, *Proceedings of the 25th IAEA Fusion Energy Conference*, Saint Petersburg, Russia , EX/P5 (2014).
[4] E. Delabie *et al.*, *Proceedings of 42nd European Physics Society Conference on Plasma Physics*, O3.113 (2015).
[5] C.F. Maggi *et al.*, *Proceedings of* 41^{st} *European Physics Society Conference on Plasma Physics*, P1.004 (2014).
[6] J.C. Hillesheim *et al.*, Physical Review Letters **116**, 065002 (2016).
[7] J.C. Hillesheim *et al.*, (to be submitted).
[8] G. Conway *et al.* Physical Review Letters **106**, 065001 (2011).
[9] T. Estrada *et al.*, Physical Review Letters **107**, 245004 (2011).
[10] G.S. Xu *et al.*, Physical Review Letters **107**, 125001 (2011).
[11] L. Schmitz *et al.*, Physical Review Letters **108**, 155002 (2012).
[12] G.R. Tynan *et al.*, Nucl. Fusion **53**, 073053 (2013).
[13] Y.R. Martin *et al.*, Journal of Physics: Conference Series **123**, 012033 (2008).